

# Numerical simulation of dynamic failure and multi spall fracture in metals

Yu V Bayandin, N V Saveleva and O B Naimark

Institute of Continuous Media Mechanics of the Ural Branch of the Russian Academy of Sciences, Academician Korolev Street 1, Perm 614013, Russia

E-mail: buv@icmm.ru

**Abstract.** Dynamic behavior of metals under intensive loading is characterized by intensive nucleation and growth of defects (microshears and microcracks) both under shock-wave compression and unloading conditions that may reduce to spallation and in some cases to multiple spallation. Spall fracture in material produced by the action of tensile stress in bulk of sample when two decompression waves collide. For higher amplitudes of shockwave the initiation of secondary spallation appears when intensity of residual wave is enough. The purpose of present investigation is consists on formulation of physical-mathematical model of dynamic behavior of metals under shock compression loadings. Plate impact test is considered. Wide range constitutive model based on the statistical theory for solids with defect (microshears and microcracks) was developed. Comparison of microstructure investigation and numerical simulation results of spall fracture (including secondary spallation) in vanadium is presented.

## 1. Introduction

Experiments on registration of shock-wave profiles by laser interferometry (VISAR) with high temporal resolution allow to study the kinetics of the elastic-plastic transition, due to the mechanism of structural relaxation in heavy accumulation of defects, plastic deformation, spall fracture and use the data to justify the wide-range constitutive equations reflecting the relationship between structural and traditional mechanical (stress, strain, strain rate) variables. Experimental studies of shock wave propagation and spall fracture were carried out during several decades [1, 2]. The investigation of spall fracture under dynamic loading and shock compression allows the estimation of different scenarios of dynamic fracture [1] including the effect of multiple spallation when the amplitude of reflected shock wave is enough for generating of secondary spall surfaces. Last studies show the increase of spall strength versus strain rate for different materials [2–5].

Using plane shock compression generators the tests were carried out for vanadium for different specimen thickness [6]. Comparison of numerical results with experimental data is proposed. Numerical results and experimental data [2, 6] concerning spallation in vanadium are presented in the figure 1. The increase of spall strength was obtained due to the strain rate hardening. The observed effect is manifested for most of investigated metals and is connected with the peculiarities of kinetics of macroscopic fracture focus (damage localization zone) occurring at much shorter times compared to the rise time of stress.



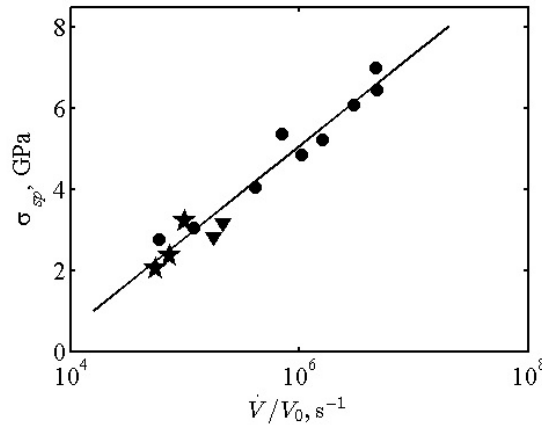


**Figure 1.** Spall strength vs strain rate ( $\blacktriangledown$ —experimental data [2],  $\bullet$ —experimental data [6],  $\star$ —numerical results [6]).

## 2. Mathematical statement

Present paper is focused on the comparison of numerical simulation results and experimental data on dynamic failure (spall) including multiple spall effect. The mathematical statement of the plane shock wave propagation in metals is proposed in papers [6–8]. The thermodynamic consistency of the model has been shown in paper [9]. Wide-range constitutive equations based on the statistical theory of mesoscopic defects were formulated in terms of defect density tensor and structural scaling parameter evolution. These variables are independent of thermodynamic parameter of non-equilibrium state of system “solid with defects” and describe multiscale damage kinetics. Structural-scaling parameters reflect the sensitivity of material to the growth of defects from the pre-existing nuclei and the current sensitivity considering the defects as activated embryos. The reaching of critical values of structural-scaling parameters is related to the failure criteria.

The system consists of kinematic relation for elastic, plastic and structural strain rate decomposition (1), balance equations (for mass (2), momentum (3) and energy (4)) and constitutive relations (5)–(8):

$$\dot{\boldsymbol{\varepsilon}} = \dot{\boldsymbol{\varepsilon}}^e + \dot{\boldsymbol{p}} + \dot{\boldsymbol{\varepsilon}}^p, \quad (1)$$

$$\dot{\rho} + \rho \nabla \cdot \boldsymbol{v} = 0, \quad (2)$$

$$\rho \dot{\boldsymbol{v}} = \nabla \cdot \boldsymbol{\sigma}, \quad (3)$$

$$\rho \dot{U} = \boldsymbol{\sigma} : \dot{\boldsymbol{\varepsilon}} - \nabla \cdot \boldsymbol{q}, \quad (4)$$

$$\boldsymbol{\sigma} = \boldsymbol{C} : \boldsymbol{\varepsilon}^e, \quad (5)$$

$$\dot{\boldsymbol{p}} = \boldsymbol{L}_1 : (\boldsymbol{\sigma} - \partial F / \partial \boldsymbol{p}), \quad (6)$$

$$\dot{\boldsymbol{\varepsilon}}^p = \boldsymbol{L}_2 : \boldsymbol{\sigma}, \quad (7)$$

$$\dot{\delta} = -L_3 \partial F / \partial \delta. \quad (8)$$

Here  $\dot{\boldsymbol{\varepsilon}} = 1/2(\nabla \boldsymbol{v} + (\nabla \boldsymbol{v})^T)$ —total strain rate tensor,  $\boldsymbol{\varepsilon}^e$ —elastic strain tensor,  $\boldsymbol{\varepsilon}^p$ —plastic strain tensor,  $\boldsymbol{p}$ —structural strain tensor (induced by microcracks and microshears),  $\rho$ —density,  $\boldsymbol{v}$ —velocity,  $\boldsymbol{\sigma}$ —total stress tensor,  $U$ —specific internal energy,  $\boldsymbol{q}$ —thermal flux (below it is neglected),  $F$ —specific free energy of solids with defects [7],  $\boldsymbol{C}$ —elastic fourth order tensor ( $\boldsymbol{C} = \lambda \boldsymbol{C}_I + 2\mu \boldsymbol{C}_{II}$ ),  $\boldsymbol{L}_1$ ,  $\boldsymbol{L}_2$  and  $L_3$ —kinetic parameters,  $\delta$ —structural scaling parameter, “.” is

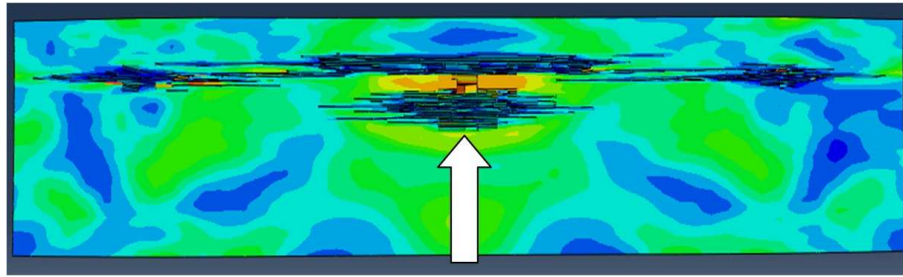


**Figure 2.** Distribution of stress at the middle cross section of sample.

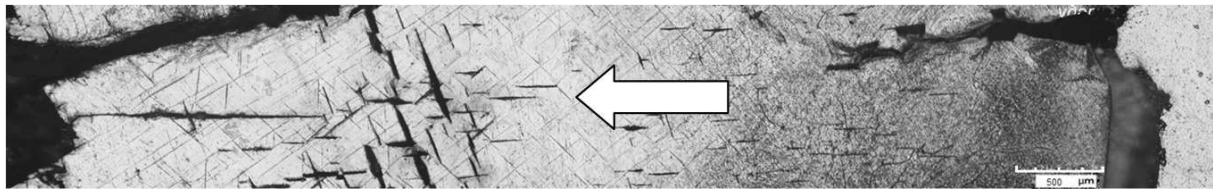


**Figure 3.** Optical image of microstructure of saved specimen.

scalar product between vectors and tensors, “:” is double scalar product between two tensors. The initial conditions for variables are taken homogeneous. The boundary conditions are applied to stress with stepped form of the input pulse  $\sigma \cdot n = f(t)$  on loading surface and  $\sigma \cdot n = 0$  on free surface.

The implementation of the developed model was based on the finite element modeling software Abaqus/Explicit using VUMAT procedure in which the mentioned system of equations (4)–(8) were formulated in the incremental form.

### 3. Results of numerical simulation

As part of developed numerical approach the influence of defects on strain hardening was separated on isotropic (microcracks) and shear (microshears) parts. In the case of spall fracture the nucleation of microcracks dominates, so it was concluded that the criteria of failure is attainment of critical values of isotropic part of defect density and stress ( $I_1(\mathbf{p}) = p_c$ ,  $I_1(\boldsymbol{\sigma}) = \sigma_c$ ). The numerical simulation was performed in three dimension case. Results of calculations are presented in the figure 2.

In the figure 2 the numerical result shows the secondary spall fracture (arrow shows the direction of shock wave propagation). This effect is linked with high values of Hugoniot elastic limit for vanadium and possibility of reverberation of the main shock wave leading to the multiple spall effect. It was also confirmed by the microstructure investigation and presented in the figure 3. Here the shock wave goes from right to left (arrow shows the direction of shock wave propagation). At the center of the picture there is the secondary spall fracture that is attended with microcracks formation.

More precisely the effect of multiple spallation was studied by the numerical simulation of the plane shock wave propagation in a quasi uniaxial state. In this case the part of sample is considered with assignments of periodic boundary conditions on its edges. The numerical simulation result shows the formation of several spall surfaces in the direction of shock wave propagation due to many reflections. The distribution of stresses and spall surfaces are shown in the figure 4. One can see fractional distribution of spall plates with thickness decreasing in zones of reflected waves. All presented numerical results allow the conclusion that the developed model adequately describes the fracture process and can describe the multiple spallation in metals.

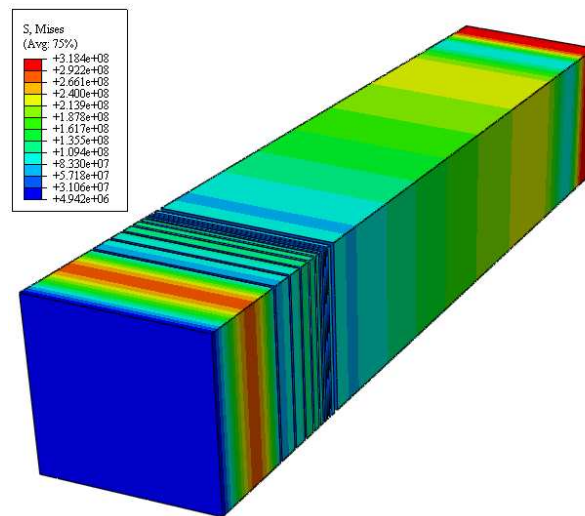


**Figure 4.** Numerical simulation results for quasi uniaxial shock wave propagation.

#### 4. Conclusions

The numerical simulation study for spall effect including multiple spallation was carried out. The increase of spall strength in vanadium was confirmed by the comparison of numerical results and experimental data published early. These results illustrate the role of essentially non-linear kinetics of defects at the final stage of damage accumulation that leads to the spall surface formation. If the amplitude of reflected shock wave is significant, then the rest of tensile stress leads to formation of secondary spall surfaces. It was shown numerically that in quasi uniaxial conditions of the plane shock wave propagation the multiple spallation appears.

#### Acknowledgments

The work was supported by program of the Ural Department of the Russian Academy of Sciences, project No. 15-10-1-18.

#### References

- [1] Meyers M A and Aime C T 1983 *Prog. Mater. Sci.* **28** 1–96
- [2] Zaretsky E B and Kanel G I 2014 *J. Appl. Phys.* **115** 243–502
- [3] Abrosimov S A, Bazhulin A P, Voronov V V, Krasnyuk I K, Pashinin P P, Semenov A Y, Stuchebryukhov I A and Khishchenko K V 2012 *Dokl. Phys.* **57** 64–66
- [4] Abrosimov S A, Bazhulin A P, Voronov V V, Geras'kin A A, Krasnyuk I K, Pashinin P P, Semenov A Y, Stuchebryukhov I A, Khishchenko K V and Fortov V E 2013 *Quantum. Electron.* **43** 246–251
- [5] Ashitkov S I, Komarov P S, Struleva E V, Agranat M B, Kanel G I and Khishchenko K V 2015 *J. Phys. Conf. Ser.* **653** 012001
- [6] Saveleva N V, Bayandin Yu V, Savinykh A S, Garkushin G V, Lyapunova E A, Razorenov S V and Naimark O B 2015 *Tech. Phys. Lett.* **41** 579–582
- [7] Saveleva N V, Bayandin Yu V and Naimark O B 2012 *Comp. Cont. Mech.* **5** 300–307
- [8] Bayandin Yu V, Naimark O B and Saveleva N V 2015 *30th International Symposium on Shock Waves: Proc. of conf.*
- [9] Kostina A A, Bayandin Yu V, Naimark O B and Plekhov O A 2014 *Key Eng. Mat.* **592–593** 205–208